

Supporting Information

Evaluating the Catalytic Contribution from the Oxyanion Hole in Ketosteroid

Isomerase

Jason P. Schwans, Fanny Sunden, Ana Gonzalez, Yingssu Tsai, and Daniel Herschlag

Material and Methods

Materials. All reagents were of the highest purity commercially available ($\geq 97\%$). All buffers were prepared with reagent grade materials or better. 5(10)Estrone-3,17-dione [5(10)EST] was from Steraloids, Inc. 5-Androstene-3, 17-dione (5-AND) was synthesized as previously described by Malhotra and Ringold and was purified by silica gel column chromatography eluting with dichloromethane as previously described by Pollack et al.^{1,2} 3-Cyclohexen-1-one was synthesized as previously described.³

KSI Mutagenesis, Expression, and Purification. Quik-Change (Stratagene) site directed mutagenesis was used to introduce the mutations into the pKSI and tKSI genes encoded on pKK22-3 plasmids or pET21c plasmids. Mutations were confirmed by sequencing mini-prep DNA from DH5a cells. Proteins were expressed and purified as previously described.⁴

KSI Kinetics. Reactions with 5(10)EST and 5-AND were monitored continuously at 248 nm in a PerkinElmer Lambda 25 spectrophotometer. Molar absorptivities of $14,800 \text{ M}^{-1}\text{cm}^{-1}$ and $14,750 \text{ M}^{-1}\text{cm}^{-1}$ were previously experimentally determined using the

commercially available products 4-estrene-3,17-dione and 4-androstene-3,17-dione, respectively.^{4,5} Reactions were conducted at 25 °C in 10 mM potassium phosphate, pH 7.2, 1 mM sodium EDTA, 2 mM DTT with 2% DMSO added as a cosolvent for substrate solubility. The values of k_{cat} , K_{M} , and $k_{\text{cat}}/K_{\text{M}}$ were determined by fitting the initial rates as a function of substrate concentration (typically eight concentrations varied from 2 to 600 mM) to the Michaelis-Menten equation. At least three determinations at differing enzyme concentration (at least fourfold overall variation) were averaged. Reactions with 3-cyclohexen-1-one were conducted as previously described.³

KSI X-ray Crystallography. Single crystal diffraction data were collected at the SSRL beamline BL9-1 using a wavelength of 0.98 Å.⁶ The reflections were indexed and integrated and with the programs *XDS*;⁷ the intensities were scaled, merged and converted to amplitudes with *SCALA* and *TRUNCATE*.⁸ The phases were derived from the PDB entry 3CPO and refined with *REFMAC5*.^{9,10} Manual model building was carried out with *COOT*.¹¹

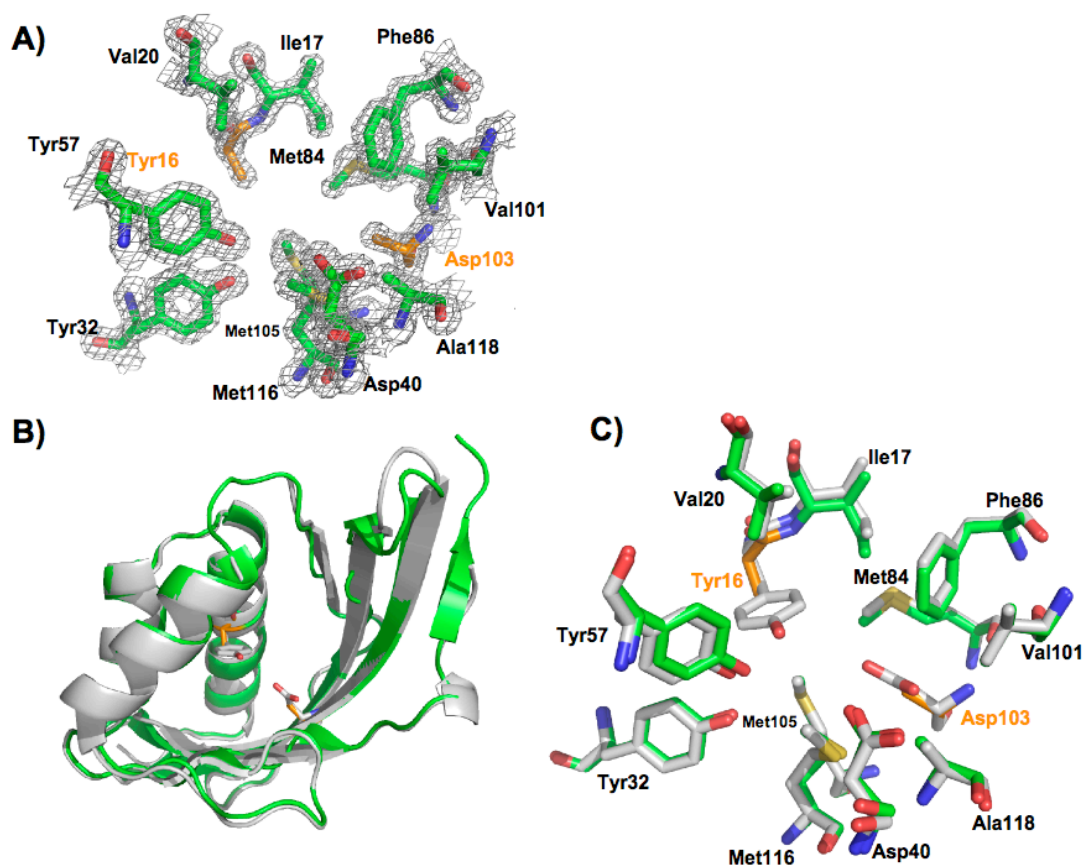
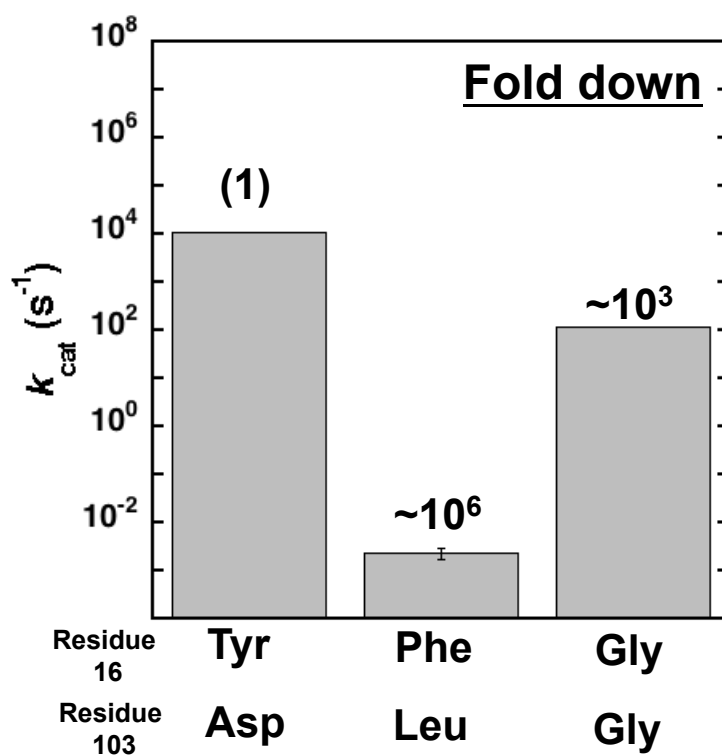
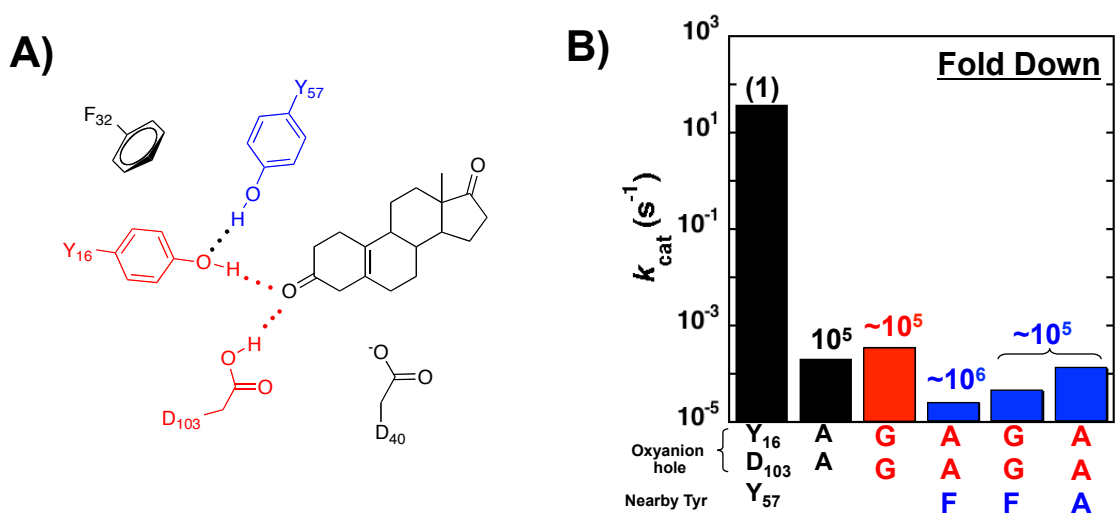


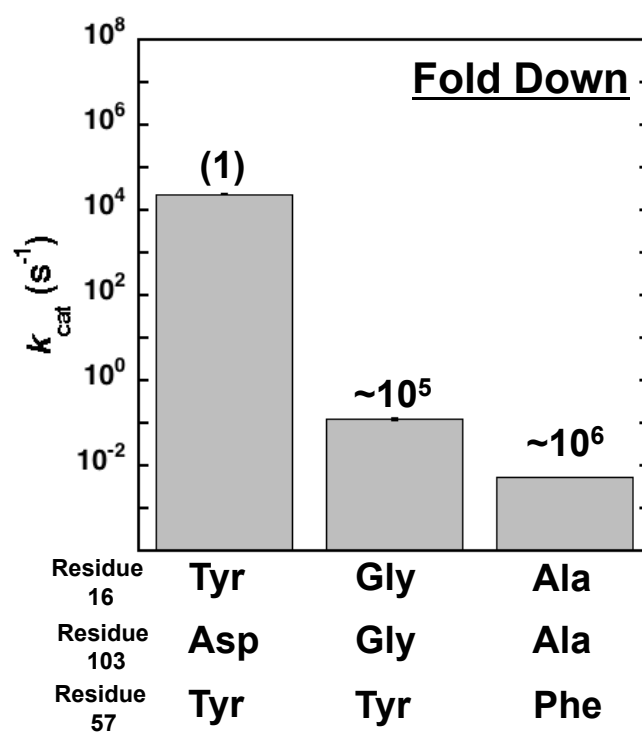
Figure S1. Overall crystal structure of pKSI Y16A/D103A is superimposable with the previously determined pKSI wild type structure. A) Sigma-A weighted $2F_o - F_c$ electron density is shown for active site residues (contoured at 2.0σ). Side chains of the mutated residues are colored orange. B) Superposition of the pKSI Y16A/D103A structure determined herein (PDB ID 3T8N, carbon atoms colored green; side chains of the mutated residues are colored orange) and the previously determined 1.9 Å pKSI wild type structure (PDB ID 1OPY, carbon atoms colored white). C) Superposition of active site residues from the structures in panel B. The overall root-mean-square deviation between the two structures for backbone atoms is 0.3 Å. X-ray data and refinement statistics are listed in Table S6.



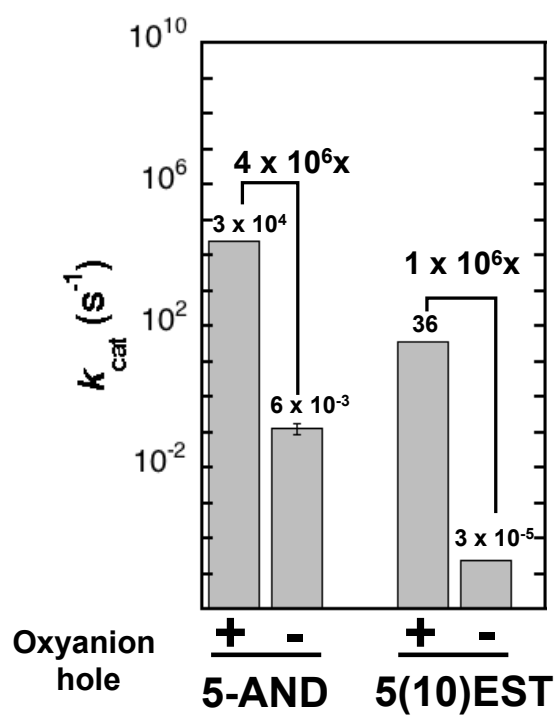
Revised Figure S2. Effects of oxanion hole mutations on pKSI activity (k_{cat}) using 5-AND. Values are averages and standard deviations from three or more independent measurements and are from revised Table S2.



Revised Figure S3. Effects of oxyanion hole mutations on tKSI activity (k_{cat}) using the steroid substrate 5(10)EST. A) Schematic representation of oxyanion hole hydrogen bond donors (red) and a nearby tyrosine (blue). B) Rate effects from mutating the oxyanion hole hydrogen bond donors and neighboring Tyr. Values and errors are averages and standard deviations from three or more independent measurements and are from revised Table S3. Bars and residues are colored according to panel A.



Revised Figure S4. Effects of oxyanion hole mutations on tKSI activity (k_{cat}) using the steroid substrate 5-AND. Values and errors are averages and standard deviations from three or more independent measurements and are from revised Table S4.



+ oxyanion hole: wt tKSI
- oxyanion hole: Y16A Y57F D103A

Revised Figure S5. Effects of oxyanion hole mutations on tKSI activity (k_{cat}) using the steroid substrates 5-AND and 5(10)EST. Values and errors are averages and standard deviations from three or more independent measurements and are from Revised Tables S3-S5. Data for S_{mini} from revised Table S5 was removed, as the rate constants were too slow to measure.

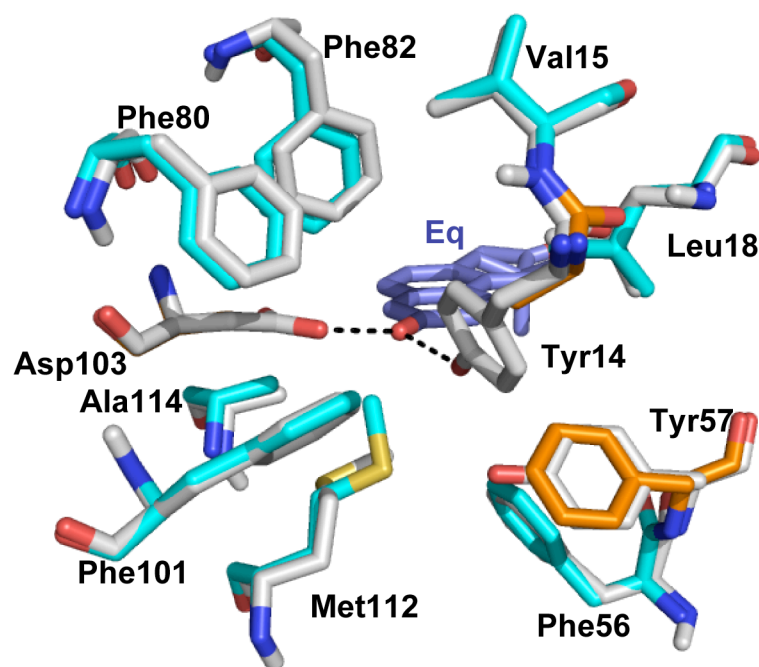
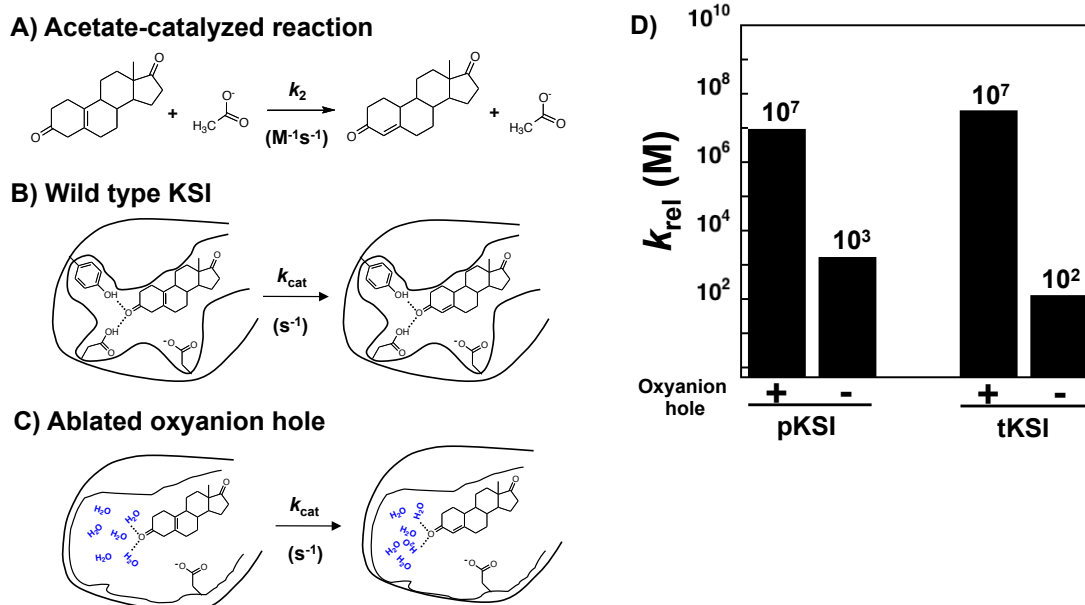


Figure S6. Superposition of the tKSI Y16A/Y57F/D103A structure determined herein (PDB ID 3T8U, carbon atoms colored cyan; side chains of the mutated residues are colored orange) and the previously determined 2.3 Å tKSI wild type structure (PDB ID 8CHO, carbon atoms colored white), and equilenin, a transition state analog, from the previously determined 2.3 Å tKSI D38N structure (PDB ID 1QJG, colored violet). X-ray data and refinement statistics are listed in Table S6.



Revised Figure S7. The catalytic contribution from KSI E•S complex relative to the acetate-catalyzed solution reaction. A) The second-order solution reaction of a KSI substrate with acetate ion. B) The first-order reaction of the wild type KSI E•S complex (k_{cat}). C) The first-order reaction of the KSI E•S complex with less-conservative smaller oxyanion hole mutations (k_{cat}). D) Comparison of the first-order enzymatic reaction with the second-order nonenzymatic acetate-catalyzed reaction provides a measure of the rate increase from the enzymatic E•S complexes relative to the solution reaction using the same general base functionality. The units for the ratio of the first-order KSI reaction with the second-order acetate-catalyzed reaction are molar (M). The values in panel D) were obtained from the following: $k_{rel} = k_{enz}/k_{ac}$; WT pKSI: $9.9 \text{ s}^{-1}/1 \times 10^{-6} \text{ M}^{-1}\text{s}^{-1} = 10^7 \text{ M}$; Y16G/D103G pKSI: $1.3 \times 10^{-3} \text{ s}^{-1}/1 \times 10^{-6} \text{ M}^{-1}\text{s}^{-1} = 10^3 \text{ M}$ (values from revised Table S1 and ref. 3); WT tKSI: $37 \text{ s}^{-1}/1 \times 10^{-6} \text{ M}^{-1}\text{s}^{-1} = 10^7 \text{ M}$; Y16G/D103G tKSI: $3.6 \times 10^{-4} \text{ s}^{-1}/1 \times 10^{-6} \text{ M}^{-1}\text{s}^{-1} = 10^2 \text{ M}$ (values from revised Table S3 and ref. 3).

Revised Table S1. Effects of oxyanion hole mutations on pKSI-catalyzed isomerization of 5(10)-EST.^a

Enzyme	k_{cat} (s ⁻¹)	K_{M} (mM)	$k_{\text{cat}}/K_{\text{M}}$ (M ⁻¹ s ⁻¹)	k_{cat} ratio (WT/mutant)	$k_{\text{cat}}/K_{\text{M}}$ ratio (WT/mutant)
Wild type	9.9 ± 0.9	30 ± 4	(3.3 ± 0.7) × 10 ⁵	[1]*	[1]*
Y16F ^b	(5.4 ± 0.1) × 10 ⁻⁴	30 ± 10	8 ± 1	19,000	70,000
Y16A ^b	(4.8 ± 0.4) × 10 ⁻²	23 ± 2	(1.5 ± 0.3) × 10 ³	200	360
Y16G ^b	(4.0 ± 0.4) × 10 ⁻²	18 ± 6	(1.7 ± 0.1) × 10 ³	250	310
Y16S ^b	(3.8 ± 0.5) × 10 ⁻²	19 ± 3	(2.2 ± 0.4) × 10 ³	260	240
Y16T ^b	(5.2 ± 0.3) × 10 ⁻²	41 ± 6	(2.7 ± 0.2) × 10 ³	190	200
D103L	(5.9 ± 0.1) × 10 ⁻²	39 ± 5	(1.5 ± 0.2) × 10 ³	170	220
D103A	(6.6 ± 0.2) × 10 ⁻²	52 ± 4	(1.3 ± 0.1) × 10 ³	150	250
D103G	(3.1 ± 0.3) × 10 ⁻¹	51 ± 13	(6.1 ± 0.9) × 10 ³	32	54
Y16F/D103L	(8 ± 2) × 10 ⁻⁶	25 ± 4	(3.2 ± 0.8) × 10 ⁻¹	1,200,000	1,000,000
Y16A/D103A	(1.1 ± 0.1) × 10 ⁻⁴	32 ± 1	(3.4 ± 0.1) × 10 ⁰	90,000	97,000
Y16G/D103G	(1.3 ± 1.2) × 10 ⁻³	36 ± 8	(3.9 ± 3.9) × 10 ¹	7600	8400
Y16G/Y57A/ D103G	7.8 × 10 ⁻⁵	603	1.3 × 10 ⁻¹	127,000	2,500,000
Y16G/Y32F/Y57A/ D103G	(1.4 ± 0.6) × 10 ⁻⁵	157 ± 35	(9 ± 2) × 10 ⁻²	700,000	3,700,000
Y16G/I28G/Y32F/Y 57A/D103G/ M116G/A118G	5.8 × 10 ⁻⁵	87	6.8 × 10 ⁻¹	170,000	500,000
Y16G/I28G/Y32F/Y 57A/F86A/ D103G/M105A/ M116G/A118G	<5.8 × 10 ⁻⁵	-	-	>170,000	-

^a Revised values are shown in red. Values for which the published and remeasured values were in agreement are shown in black.

^b Values from Kraut et al.⁴

* Defined as unity for comparison.

Standard deviations from at least three experiments at different enzyme concentrations are given in parentheses.

Revised Table S2. Effects of oxyanion hole mutations on pKSI-catalyzed isomerization of 5-AND.^a

Enzyme	k_{cat} (s ⁻¹)	K_{M} (mM)	$k_{\text{cat}}/K_{\text{M}}$ (M ⁻¹ s ⁻¹)	k_{cat} ratio (WT/mutant)	$k_{\text{cat}}/K_{\text{M}}$ ratio (WT/mutant)
Wild type	1.1×10^4	81	1.4×10^8	[1]*	[1]*
Y16F/D103L	$(2.3 \pm 0.6) \times 10^{-3}$	13 ± 1	$(1.7 \pm 0.5) \times 10^2$	4,800,000	820,000
Y16G/D103G	$(1.2 \pm 0.1) \times 10^1$	89 ± 30	$(1.4 \pm 0.5) \times 10^5$	900	1000

^a Revised values are shown in red. Values for which the published and remeasured values were in agreement are shown in black.

* Defined as unity for comparison.

Standard deviations from at least three experiments at different enzyme concentrations are given in parentheses.

Revised Table S3. Effects of oxyanion hole mutations on tKSI-catalyzed isomerization of 5(10)-EST.^a

Enzyme	k_{cat} (s ⁻¹)	K_{M} (mM)	$k_{\text{cat}}/K_{\text{M}}$ (M ⁻¹ s ⁻¹)	k_{cat} ratio (WT/mutant)	$k_{\text{cat}}/K_{\text{M}}$ ratio (WT/mutant)
Wild type	37 ± 2	28 ± 4	(1.3 ± 0.2) × 10 ⁶	[1]*	[1]*
Y16A/D103A	(2.0 ± 0.4) × 10 ⁻⁴	39 ± 7	(5.0 ± 0.2) × 10 ⁰	185,000	260,000
Y16G/D103G	(3.6 ± 0.7) × 10 ⁻⁴	40 ± 5	(9 ± 3) × 10 ⁰	100,000	140,000
Y16A/Y57F/D103A	2.5 × 10 ⁻⁵	30	8.4 × 10 ⁻¹	1,500,000	1,500,000
Y16G/Y57F/D103G	4.5 × 10 ⁻⁵	23	2.0 × 10 ⁰	820,000	650,000
Y16A/Y57A/D103A	(1.3 ± 0.2) × 10 ⁻⁴	17 ± 2	(8 ± 0.2) × 10 ⁰	280,000	160,000

^a Revised values are shown in red. Values for which the published and remeasured values were in agreement are shown in black.

* Defined as unity for comparison.

Standard deviations from at least three experiments at different enzyme concentrations are given in parentheses.

pKSI numbering is used throughout.

Revised Table S4. Effects of oxyanion hole mutations on tKSI-catalyzed isomerization of 5-AND.^a

Enzyme	k_{cat} (s ⁻¹)	K_{M} (mM)	$k_{\text{cat}}/K_{\text{M}}$ (M ⁻¹ s ⁻¹)	k_{cat} ratio (WT/mutant)	$k_{\text{cat}}/K_{\text{M}}$ ratio (WT/mutant)
Wild type	$(2.4 \pm 0.1) \times 10^4$	160 ± 33	$(1.5 \pm 0.1) \times 10^8$	[1]*	[1]*
Y16G/D103G	$(1.3 \pm 0.1) \times 10^{-1}$	154 ± 24	$(1.3 \pm 1.1) \times 10^3$	180,000	120,000
Y16A/Y57F/D103A	5.6×10^{-3}	139	4.0×10^1	4,300,000	3,800,000

^a Revised values are shown in red. Values for which the published and remeasured values were in agreement are shown in black.

* Defined as unity for comparison.

Standard deviations from at least three experiments at different enzyme concentrations are given in parentheses.

pKSI numbering is used throughout.

Revised Table S5. Effects of oxyanion hole mutations on tKSI-catalyzed isomerization of 3-cyclo-hexen-1-one (S_{mini})^a

Enzyme	k_{cat} (s ⁻¹)	K_{M} (mM)	$k_{\text{cat}}/K_{\text{M}}$ (M ⁻¹ s ⁻¹)	k_{cat} ratio (WT/mutant)	$k_{\text{cat}}/K_{\text{M}}$ ratio (WT/mutant)
Wild type	$(1.7 \pm 0.2) \times 10^1$	278 ± 30	$(6.2 \pm 0.1) \times 10^1$	[1]	[1]

Y16A/Y57F/D103A

^a Data for reaction of S_{mini} and Y16A/Y57F/D103A were omitted in the revised table as the reaction was too slow to measure.

Standard deviations from at least three experiments at different enzyme concentrations are given in parentheses for the wild type measurement.

pKSI numbering is used throughout.

Table S6. Crystallographic Data-Collection and Refinement Statistics		
	All Data (Outer shell)	
Data Set	pKSI Y16A/D103A	tKSI Y16A/Y57A/D103A
PDB ID	3T8N	3T8U
Resolution Range (Å)	38.3-1.47 (1.50-1.47)	35.1-2.50 (2.57-2.50)
Space Group	C121	P6 ₁ 22
a, Å	127.5	64.2
b, Å	76.7	64.2
c, Å	53.1	497.0
a, °	90.0	90.0
b, °	64.0	90.0
g, °	90.0	120.0
Number Unique Reflections	77108 (10103)	22525 (30061)
Completeness	98.0 (88.4)	99.5 (97.0)
Multiplicity	3.6 (3.2)	10.5 (6.8)
R _{merge} , %	3.8 (87.2)	7.7 [111.6 (because of the multiplicity)]
I/s	18.0 (1.3)	21.9 (1.6)
Refinement Statistics		
No. Residues	130	123
No. Waters	214	88
R _{work} , %	17.7 (39.1)	23.9 (34.5)
R _{free} , %	21.8 (40.3)	30.9 (44.6)
rmsd bond, Å	0.016	0.012
rmsd angle, °	1.521	1.33
$R_{merge} = \frac{\sum_{hkl} \sum_i I(hkl)_i - \{I(hkl)\} }{\sum_{hkl} S_i I(hkl)_i}$ $R_{work} = \frac{\sum_{hkl} F(hkl)_o - \{F(hkl)_c\} }{\sum_{hkl} F(hkl)_o}$ <p>R_{free} was calculated exactly as R_{work} where $F(hkl)_o$ were taken from 10% of the data not included</p>		

Supporting Information References

- (1) Pollack, R. M.; Zeng, B.; Mack, J. P. G.; Eldin, S. *J. Am. Chem. Soc.* **1989**, *111*, 6419-6423.
- (2) Malhotra, S. K.; Ringold, H. J. *Tetrahedron Letters* **1962**, *3*, 669-672.
- (3) Schwans, J. P.; Kraut, D. A.; Herschlag, D. *Proc. Natl. Acad. Sci. U.S.A.* **2009**, *106*, 14271-14275.
- (4) Kraut, D. A.; Sigala, P. A.; Fenn, T. D.; Herschlag, D. *Proc. Natl. Acad. Sci. U.S.A.* **2010**, *107*, 1960-1965.
- (5) Kraut, D. A.; Churchill, M. J.; Dawson, P. E.; Herschlag, D. *ACS Chem. Biol.* **2009**, *4*, 269-273.
- (6) Soltis, S. M.; Cohen, A. E.; Deacon, A.; Eriksson, T.; Gonzalez, A.; McPhillips, S.; Chui, H.; Dunten, P.; Hollenbeck, M.; Mathews, I.; Miller, M.; Moorhead, P.; Phizackerley, R. P.; Smith, C.; Song, J.; van dem Bedem, H.; Ellis, P.; Kuhn, P.; McPhillips, T.; Sauter, N.; Sharp, K.; Tsyba, I.; Wolf, G. *Acta Crystallogr. D Biol. Crystallogr.* **2008**, *64*, 1210-1221.
- (7) Kabsch, W. *Acta Crystallogr. D Biol. Crystallogr.* **2010**, *66*, 125-132.
- (8) Collaborative Computational Project, N. *Acta Crystallogr. D Biol. Crystallogr.* **1994**, *50*, 760-763.
- (9) Murshudov, G. N.; Vagin, A. A.; Dodson, E. J. *Acta Crystallogr. D Biol. Crystallogr.* **1997**, *53*, 240-255.
- (10) Krissinel, E. B.; Winn, M. D.; Ballard, C. C.; Ashton, A. W.; Patel, P.; Potterton, E. A.; McNicholas, S. J.; Cowtan, K. D.; Emsley, P. *Acta Crystallogr. D Biol. Crystallogr.* **2004**, *60*, 2250-2255.
- (11) Emsley, P.; Cowtan, K. *Acta Crystallogr. D Biol. Crystallogr.* **2004**, *60*, 2126-2132.
- (12) Choi, G.; Ha, N. C.; Kim, S. W.; Kim, D. H.; Park, S.; Oh, B. H.; Choi, K. Y. *Biochemistry* **2000**, *39*, 903-909.